Bachelor Project

Czech Technical University in Prague

F3

Faculty of Electrical Engineering
Department of Measurement

Unit for Vibrating Sample Magnetometer

Patrick Theodore P. Ramos

Supervisor: doc. Ing. Mattia Butta, Ph.D.
August 2020

BACHELOR'S THESIS ASSIGNMENT

I. Personal and study details

Student's name: **Ramos Patrick Theodore** Personal ID number: **472231**

Faculty / Institute: **Faculty of Electrical Engineering**

Department / Institute: **Department of Electrical Power Engineering**

Study program: **Electrical Engineering and Computer Science**

II. Bachelor's thesis details

Bachelor's thesis title in English:

Unit for Vibrating Sample Magnetometer

Bachelor's thesis title in Czech:

Přístroj pro Vibrating Sample Magnetometer

Guidelines:

Vibrating Sample Magnetomete (VSM) is a powerful method for characterising quasi-static properties of ferromagnetic material.
VSMs are typically very expensive because they must include a large yoke for generation of large and static magnetic field and lock-in amplifier for demodulation of the voltage induced in the pick-up coil.
In our laboratory we already have both these instruments, therefore we can create a very inexpensive VSM by adding a simple vibrating mechanism above the yoke and synchronising it to a lock-in amplifier.
This would increase the characterisation capability of our laboratory for very little expense.
The student:
- will design the shape and number of turns of the pick-up coil by calculating (using FEM) the required parameter necessary to obtain the minim induced voltage using typical magnetic sample.
- will create and assemble the coil
- will adapt commercially available vibrating system to the yoke
- will programme a software in Labview for creation of magnetic field and reading measurement from the lock-in amplifier.

Bibliography / sources:

Name and workplace of bachelor's thesis supervisor:

doc. Ing. Mattia Butta, Ph.D., Department of Measurement, FEE

Name and workplace of second bachelor's thesis supervisor or consultant:

Date of bachelor's thesis assignment: **28.02.2020** Deadline for bachelor thesis submission: **14.08.2020**

Assignment valid until: **19.02.2022**

doc. Ing. Mattia Butta, Ph.D. Supervisor's signature	Head of department's signature	prof. Mgr. Petr Páta, Ph.D. Dean's signature

III. Assignment receipt

The student acknowledges that the bachelor's thesis is an individual work. The student must produce his thesis without the assistance of others, with the exception of provided consultations. Within the bachelor's thesis, the author must state the names of consultants and include a list of references.

.	
Date of assignment receipt	Student's signature

Acknowledgements

I would like to thank the following for their help in this study:

My advisor doc. Ing. Mattia Butta Ph.D. Who offered me the challenge to take on this project and has constantly been driving me to learn, do better and improve past my current capabilities.

The Institute of Material Science of CSIC Madrid for lending us the use of their Microsense EV11 VSM.

prof. Ing. Pavel Ripka, CSc. for allowing us the opportunity to test the VSM design with nanowire samples provided by him.

Ing. David Novotný for 3D printing the models we designed.

My dear, Dasha, for all her kindness and support.

Mr. Byron Schutte for lending me instruments for testing and fabricating the PCB during the quarantine period.

My parents who have worked hard and sacrificed much so my brother and I could have the opportunity to live and study abroad.

The Filipino People, who I hope to serve well in the future.

Ad Majorem Dei Gloriam

Declaration

I declare that this work is all my own work and I have cited all sources I have used in the bibliography.

Prague, August 11, 2020

Prohlašuji, že jsem předloženou práci vypracoval samostatně, a že jsem uvedl veškerou použitou literaturu.

V Praze, 11. srpna 2020

Abstract

The aim of this thesis was to develop a proof of concept for building a low-cost Vibrating Sample Magnetometer(VSM) using an Arduino-based PCB and instruments already available in the University's laboratories. This device was constructed to serve as a substitute to purchasing an expensive, commercially available VSM. In this this thesis, you can find the operating principle of a VSM and an overview of how the hardware and software of the prototype for the low-cost VSM were designed to replicate it. Furthermore, it is explained how the feasibility of the design for practical use was tested in terms of signal-to-noise ratio and comparison to measurements of the magnetic hysteresis of CoFeSiB amorphous wires obtained with a Microsense EV11 commercial VSM.

Keywords: Vibrating Sample Magnetometer, Low-cost, magnetic measurements

Supervisor: doc. Ing. Mattia Butta, Ph.D.
Faculty of Electrical Engineering
Technická 2 166 27 Praha 6 - Dejvice

Abstrakt

Cílem této bakalářské práce bylo vyvinutí důkazu konceptu pro sestavování levného Vibračního vzorkovacího magnetometru (VSM) za použití Arduino desek s tištěnými obvody (PCB) a přístrojového vybavení dostupného v univerzitních laboratořích. Toto zařízení bylo zkonstruováno jako alternativa k zakoupení dražších, komerčně prodávaných VSM. Tato práce obsahuje principy fungování VSM a popis návrhu hardwaru a softwaru pro prototyp levného VSM, podle kterého jej lze sestavit. Dále tato bakalářská práce popisuje jak byla testována vhodnost návrhu pro praktické použití z hlediska porovnání síly původního signálu oproti šumu (SNR) a porovnáním měření s měřeními magnetické hystereze CoFeSiB amorfních drátků pomocí Microsense EV11, komerčního VSM.

Klíčová slova: Vibrating Sample Magnetometer, levný, magnetická měření

Překlad názvu: Přístroj pro Vibrating Sample Magnetometer

Contents

Figures

Tables

Chapter 1

Introduction

The measurement of magnetic hysteresis characteristics of materials is crucial in determining their magnetic properties such as their remanence, coercivity, and saturation magnetization[1-4]. These characteristics are also necessary for classifying ferromagnetic and ferrimagnetic materials as soft or hard magnetic materials[4-6]. This classification is important when testing the efficiency of wires and other electronic components as the size of a material's hysteresis corresponds to its magnetic losses[4-5].

Typically, the magnetic hysteresis characteristic can be measured by fully magnetizing and demagnetizing a sample in both directions while measuring the magnetic induction B of the sample vs. the applied field H. This B is proportional to the magnetic moment of the sample; how much its magnetic dipoles are oriented with respect to the applied field[4-5]. The magnetic moment of the sample could be measured using the standard induction-based measurement method. Wherein, the integral of the voltage induced in a pickup coil wound around a sample is used as a measure of the magnetic flux arising from the sample as it is subjected to a changing magnetization field.

This method has two limitations. The first is that if the measurement has to be conducted at a low frequency, the signal from the pickup coil would be small enough to be comparable to the background noise. The second is that this method is not suited for measuring very small samples. It would be difficult enough to wind a pickup coil for a 3mm piece of wire and it would be impossible to do so for nanowires.

Instead, the Vibrating Sample Magnetometer (VSM), first proposed by Foner in 1955[7], is what is commonly used to measure the magnetic moment of materials. Rather than using a stationary setup with a changing applied field, he proposed to have a fixed pickup coil and have the sample be oscillated sinusoidally while immersed in a DC magnetic field. Foner's original proposal was simple, using only a magnet, a straw, a speaker and a paper cup[7]. Over the years it has improved and developed into the commercially produced VSMs on the market today. Only a few companies produce these VSMs, and even second-hand VSMs are sold at a price of about 100,000 to 900,000 Kč.

The possession of a VSM would prove useful to the department for the measurement of the magnetic characteristics of some small samples of material. The cost of purchasing one could be deemed unreasonable though since some

instruments used in the commercial VSM designs, such as power supplies, an electromagnet and a lock-in amplifier are already readily available in the University's laboratories. It would be better to construct a functioning VSM for a lower cost by using these instruments from the laboratory.

The goal of our study is to produce a proof of concept for this notion. We intend to build a prototype for a low-cost DIY VSM using instruments already available in the laboratory in conjunction with an Arduino-based control PCB and to write a LabVIEW user interface software to control it. The feasibility of this design being used as an alternative to purchasing or borrowing a commercial VSM would then have to be determined. This will be done using the hysteresis data of a sample of CoFeSiB amorphous wire obtained using a Microsense EV11 VSM borrowed from the Institute of Material Science of CSIC Madrid as a point of comparison of measurement quality.

Chapter 2

Theory

The measurement of magnetization of a sample is usually based on Ampere and Lenz's laws. [8] In the classical induction-based measurement method, a sample is placed in the air gap within a wound pickup coil. These are both then placed within a larger coil that applies a time-varying magnetic field to them. This orients the magnetic dipoles within the sample which produces its own magnetic field whose flux passes through the pickup coil. The voltage induced in the pickup coil by a time-varying magnetic field can be integrated to derive this flux. This flux and the dimensions of the sample can then be used to calculate the magnetic induction of the sample[5,8].

There are two problems with this method. First is that the total measured magnetic flux will be a sum of the flux due to the air and the flux due to the sample. This entails that the coil must be closely wound around the sample so that the offset of the flux due to the area of air in the coil vs. the area of the sample remains much smaller than the flux due to the sample. This gets increasingly more difficult depending on how small the sample is since there is a limit to how closely a coil can be wound. Second, is that for some samples, it is necessary to measure the quasi-static properties of the material, and so, the sample must be exposed to a DC field instead. This entails that the absence of a time varying field would cause no voltage to be induced in the pickup coil.

Thus, for these cases, instead of using classical induction-based measurements, it would be necessary to use a form of Foner's Vibrating Sample Magnetometer(VSM)[7]. Instead of applying a time-varying magnetic field, a VSM uses displacement to create a time-variation of flux relative to the fixed measurement position of the pickup coil. A rod attached to a vibrator sinusoidally oscillates the sample between a position in front of the coil and displaced from it. As the magnetized sample moves, so does the magnetic field arising from it[7]. Since the flux at a point is dependent on the displacement from the source of magnetic field, this creates the time-varying magnetic flux in the pickup coil needed to generate the measurable current. The VSM takes a direct measurement of magnetization M by measuring the difference in magnetic induction between when the sample is present or absent in the space in front of the pickup coil. [5]

The signal taken from the coil will be an AC signal with its frequency

fixed to that of the vibrator. This signal would be buried in high-frequency noise and will need to be demodulated by a lock-in amplifier(LIA) which requires a reference signal similar in frequency to the vibrator signal[9,10]. The lock-in amplifier would then multiply the input signal by this reference to filter out the external noise and extract the real part of this signal. This will then serve as the output of the system and can then be interpreted as a measure of the sample's magnetization for the specific value of applied magnetic field. These measurements are then taken in sequential steps of applied field until the sample has been fully magnetized and demagnetized in both directions. They can then be plotted together to measure the magnetic hysteresis loop of the sample. From the obtained hysteresis loop, we can then quantify the magnetic properties of the sample such as its coercivity, remanence, saturation magnetization and its magnetic losses[1-2, 5-6, 11].

Chapter 3

Implementaion

3.1 Overview of Design

Our goal is for the low-cost VSM to function like a commercially manufactured VSM and produce magnetic hysteresis measurements of comparable quality to it. It will be built using an Arduino-based control PCB connected to the instruments that were already present in the labs of the University. Control of the VSM's settings, communications with the parts on the PCB, and the collection and interpretation of data would then be accessible to the user through the control panel of a LabVIEW program.

Our PCB must then perform the following tasks:

- Production of the applied magnetic field and accurate measurement of it
- Controlling the movement of the sample using the vibrator
- Measuring the moment of the sample using a pickup coil and a LIA
- Facilitating user control and processing of data

Each of which are depicted briefly in the following flowchart and will be described in depth in the next sections.

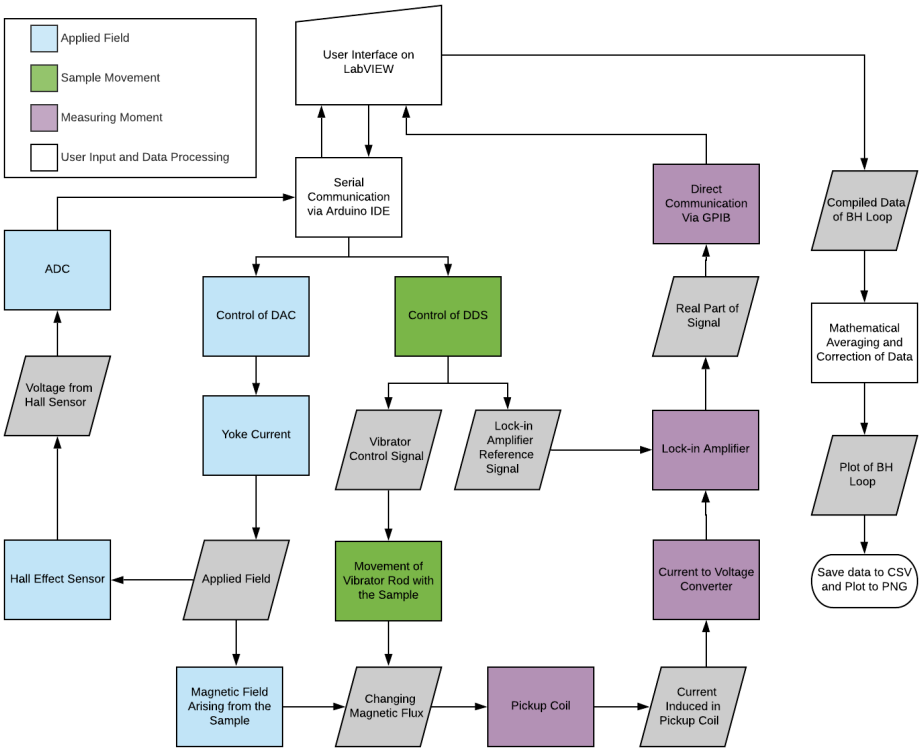

Figure 3.1: Flowchart of the Processes Involved in the Operation of the VSM

3.2 Production of Applied Field

The first issue that had to be tackled was how to produce the magnetic field that will be applied to the sample. This field had to be uniformly applied over the area wherein the full range of the sample's movement occurs. It had to be finely controllable such that the field can be changed by small increments near the transition of the hysteresis loop. It also had to be applicable in both a positive and negative direction to fully magnetize and demagnetize the sample when measuring hysteresis. Lastly, the field strength would have to be precisely measured each time it is changed.

For our VSM, a magnetic yoke from the University's magnetics laboratory was used to generate the applied field.

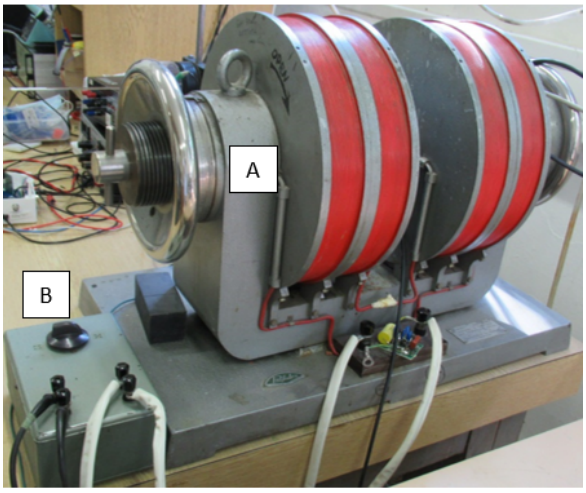

Figure 3.2: The Yoke

With a diameter of 98 mm, the area of its poles are sufficiently large enough compared to the sample and area of the pickup coil (5mm). The applied field within the area of the full range of motion of the sample (5 mm) could thus be considered uniform. These large poles and adjustable air gap were also beneficial as it allowed for easy installment and adjustment of position of the pickup coil and the vibrator. (A)

The yoke generated a magnetic field based on current values set on the controls of its power supply. It also had a manual control for switching polarity, that allows it to apply a magnetizing and demagnetizing field to each sample. (B)

The current in the yoke used to produce the field is controllable manually but can also be set to be piloted remotely by analog signals sent via coaxial cable. The latter was used in the design of the VSM as it would allow us to use a control program to precisely set the applied field to a chosen set of values automatically.

Figure 3.3: The DAC

Therefore, to automate the setting of applied field, we decided to use a DAC to control the power supply of the yoke. The size of the DAC's LSB would dictate the smallest change in field Δ H that can be set in the yoke and the product of the LSB and the DAC's maximum range would dictate the maximum field that can be set in the yoke H_{max}. This thus presents us with a trade-off between precision and range.

In order to get a high quality hysteresis loop and a good measurement

of coercivity, it is necessary to have more measurements taken at smaller steps near the transition of the loop. It would still be necessary to have some measured points past saturation, but not as many. Thus, smaller steps of ΔH should be prioritized over being able to apply field over a large range.

An MCP4725 DAC was selected to control the yoke's power supply. The MCP4725 is a low power, high accuracy DAC that requires a 5V power source as its VDD. It was selected for use specifically for its 12-bit resolution allowing for a code range between 0 and 4095 and an ideal LSB of 1.22 mV. [12] After some measurements, it was found that the LSB of 1.22 mV corresponds to a ΔH of $\approx$ 143 A/m.

This LSB was still too large. Therefore, we had to reduce the produced voltage from the DAC. We designed a circuit at the output of the DAC that would amplify the voltage by a factor of 0.122. Which would have the LSB correspond to a ΔH of $\approx$ 17.5 A/m allowing for even more precise setting of applied field strength.

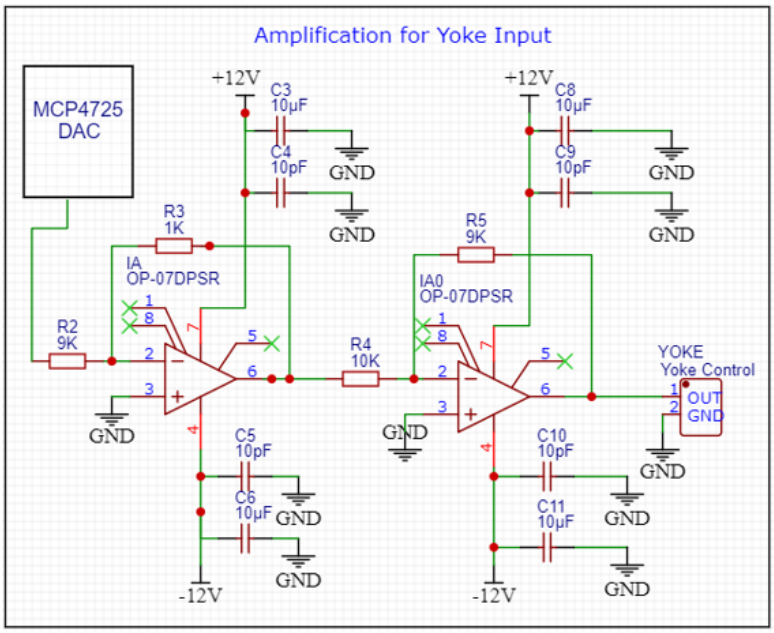

Figure 3.4: The Schematic of the Amplification Circuit of the DAC Output

After the output of the DAC, an OP07 was set up as an inverting amplifier with a gain of -0.11. An inverting amplifier was used since, unlike the non-inverting amplifier, it can provide a fractional gain since its gain range starts from 0 and not 1. A second OP07 was then set as an inverting amplifier with a gain of -1.11 since the remote control of the yoke's power supply only accepts positive input. These resulted in a final gain of 0.122 at the output of the amplification circuit.

For the sake of noise reduction, the following measures were taken:

- Bypass capacitors of different values were placed in parallel with each other on the power rails of the OP07s as to reduce power supply noise

in a wide frequency range.

- A shielded BNC cable was used as the connection between the output of the circuit and the yoke's remote control input to reduce noise from the environment of the room.

We had to then consider the effect of this de-amplification on the range of field values that the yoke can produce under this control. The CoFeSiB amorphous wires measured using the Microsense EV11 VSM reached saturation at around 2×10^4 A/m and points were still measured in the saturated region until 7×10^5 A/m. Since these wires will be the main baseline for comparison between our VSM and the commercial VSM, the maximum range of field must be at least larger than 2×10^4 A/m. The field produced at a DAC value of 4000, near its maximum range, was observed to be 8.6×10^4 A/m. Thus, the range of field values is still sufficient for our purposes even after de-amplifying the output of the DAC.

Lastly, this system would need a means of accurately measuring the applied field. This could be done by means of a calibration of the DAC codes or by measuring the current in the yoke. These options were ruled out though since the yoke has a ferromagnetic core with its own hysteresis that may not be negligible.

The baseline comparison for our proof-of-concept is hysteresis data of CoFeSiB amorphous wires measured by the commercial VSM. Therefore, negligibility of the yoke hysteresis would be evaluated based on its size relative to the measured coercivity of the CoFeSiB amorphous wire 16.4 A/m.

To do this, a Lakeshore 450 Gaussmeter was used to measure the field in the yoke at different values of current. The gaussmeter probe was placed between the yoke poles in line with the position of the pickup coil and the hall effect sensor. The current was then adjusted to give field values ranging from about -105 mT to 105 mT and resulted in the following characteristic:

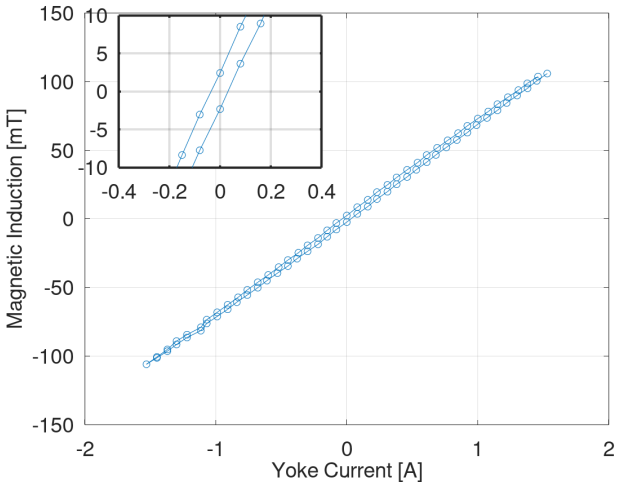

Figure 3.5: Characteristic of the Measured Field vs the Current in the Yoke

We can see here that the current in the yoke has a non-linear relationship with the field applied by the yoke to the sample. This was expected since the yoke's ferromagnetic core would have its own hysteresis. This hysteresis was calculated to be 3779 A/m. Compared to the coercivity of the CoFeSiB amorphous wire 16.4 A/m, this is large, and would create a non-linearity that will not be tolerable. Thus, it would not be sufficiently precise to measure the applied field using the current in the yoke. Instead, an SCE SS49e hall effect sensor would be used to directly measure the applied field.

To hold the hall sensor in the yoke, the mount seen in figs 3.6 and 3.7 was designed in SketchUp and 3D printed. It was made to be easily installed on one side of the yoke and would hold both the pickup coil and the hall sensor. The hall sensor was epoxied in the groove of the mount with its sensing side facing outwards. It was then connected to the main PCB via an aux cable.

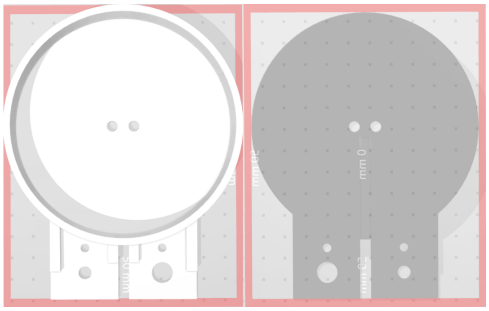

Figure 3.6: SketchUp Model of the Coil Mount

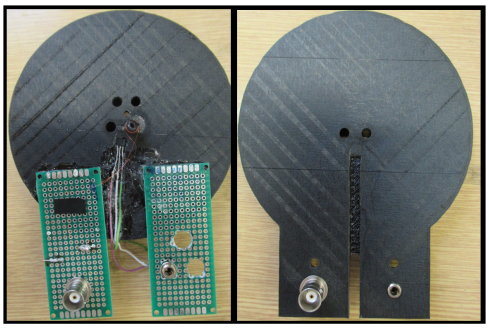

Figure 3.7: Prototype Coil Mount and Coil Mount for Future Use

Before the hall sensor could be used for the VSM, it would first have to be calibrated using the gaussmeter. The gaussmeter probe was placed in the same position as in the last measurement, and field values were applied in a range from -200 mT to 200 mT resulting in the following characteristic:

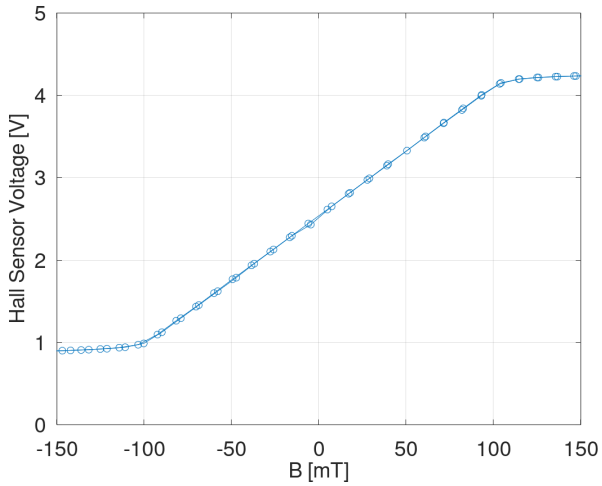

Figure 3.8: Voltage-Field Characteristic of the Hall Effect Sensor

We can see here that within the range of about -100 mT to 100 mT, relationship between the applied field and the measured field is linear. Thus, the hall sensor allows us to measure the field applied by the yoke without the hysteresis of the yoke's ferromagnetic core interfering with the readings.

If the points within the linear range of the hall sensor are extracted from this data set, the following characteristic can be obtained.

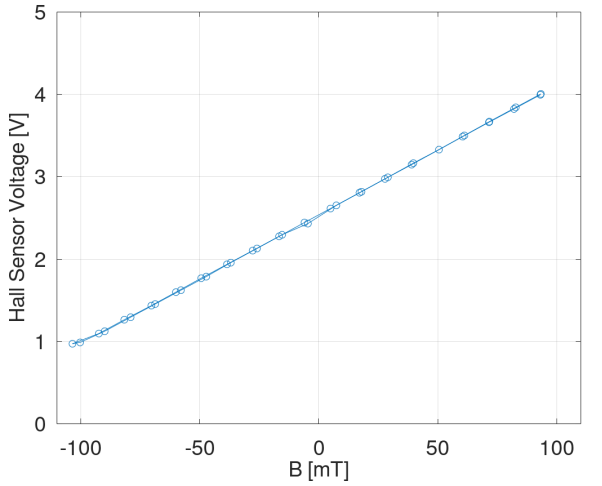

Figure 3.9: Linear Region of the Hall Sensor's Characteristic

Linear approximation can be then applied to find a conversion equation between the voltage output of the hall sensor and the measured field. It was found that the measured values have a voltage offset of 2.5389 V and the sensor has a measured sensitivity of 15.67 V/T. These can then be used in the calibration of the hall effect sensor:

$$H[A/m] = \frac{Voltage[V] - 2.5389[V]}{15.67[V/T]} \times \frac{1}{\mu_0[H/m]} \tag{3.1}$$

For later practical use of the VSM, a standard sample of known values will have to be measured to calibrate the instrument through the use of adjustable multiplicative and additive conversion factor controls included in the control program.

Once calibrated, the output of the hall sensor would then have to be read by an ADC. Since it has a sensitivity of 15.67 V/T, ideally, the ADC will need to have an LSB that is at least in the same order of magnitude of 10 μV. Though an ADC with a lower resolution will be sufficient to measure the value of H each time the field is changed, the ADS1256 Delta-Sigma ADC was used since it was readily available in the lab. It has a 24-bit resolution which results in an LSB of 11.97 μV[13].

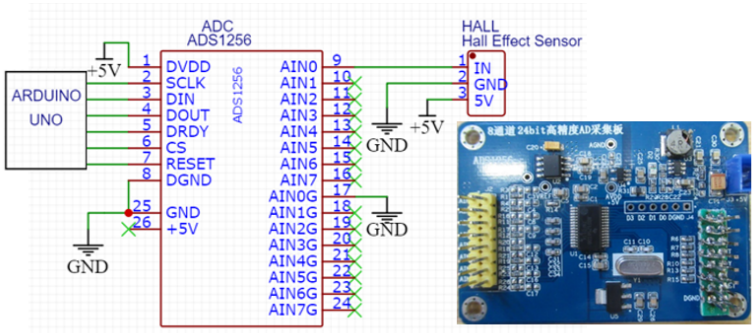

Figure 3.10: Sample and Schematic of the ADS1256 ADC

3.3 The Vibrator

As stated earlier, the core of the VSM's working principle is the time variation of magnetic flux seen by the coil is created by the movement of the sample[5,7]. Now that we have a means of generating, controlling and measuring the applied a magnetic field, we can then shift our focus to securing the sample and vibrating it within this field.

First, it was necessary to address how to attach the sample securely to the vibrator. It had to be taken into account that the sample holders used in VSMs must not introduce any non-negligible changes to the magnetic field. They are commonly made of non-magnetic materials such as quartz or brass[14,15]. The sample must also be secured on the holder with the use of non-magnetic materials such as 2-part epoxy, GE7031 Varnish, Kapton Tape or Teflon Tape [14,15]. For our purposes, glass rods with a flat end were fabricated as sample holders and Teflon tape was used to secure the samples on this flat end.

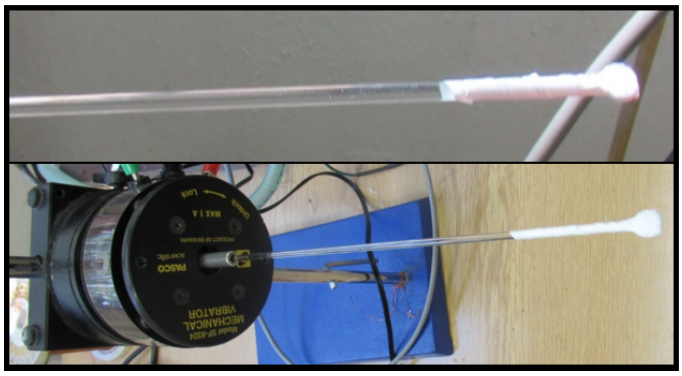

Figure 3.11: Securing of the CoFeSiB Amorphous Wire to the Sample Holder and Vibrator

As for the movement of the sample, a PASCO SF-9324 Variable Frequency Mechanical Wave Driver was chosen as the vibrator for the following reasons.

It has an attached drive arm that the sample holder can easily be affixed to. Allowing for easy installment and removal of samples.

Its mechanical wave driver is controllable by a signal from a waveform generator and can vibrate with any frequency within a range of 0.1 Hz to 5 kHz[16]. This makes it possible to easily change the frequency of the sample's vibration if the waveform generator is programmable via serial communication with the Arduino.

The datasheet for the vibrator also states that its amplitude remains consistently at 5mm up to 50Hz[16]. It was observed that changing the vibrator frequency within this range did not cause a variation in the amplitude of the sample's motion. This was only done though through optical observation though as we lacked the means necessary to properly quantify this effect.

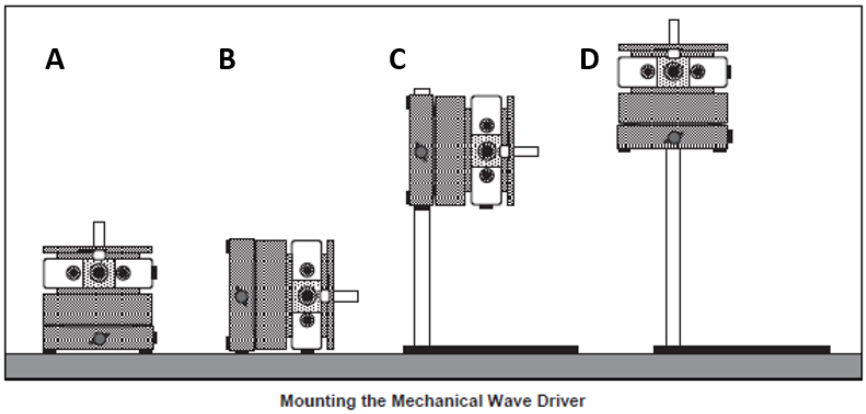

Figure 3.12: Operating Positions for the Vibrator Shown in its Data Sheet[16] (Source: PASCO Scientific 1990)

As seen in the image, it can function horizontally while mounted on a 1.27 cm rod. Position C was chosen for our purposes because there is no space in the bottom of the yoke to fit a vibrator so the sample would have to be placed

into the air gap from the side. Mounting from the side on a rod also allows for easier adjustment of the sample's height and position without having to change the length of the sample holder.

Once the vibrator and sample holders were purchased and installed, it was time to design the circuit for the waveform generator that will drive them. We selected the CJMCU AD9833 Direct Digital Synthesis (DDS) waveform generator to produce sinusoidal signal that will be used both to control the vibrator's movement and to serve as the reference for the lock-in amplifier later.

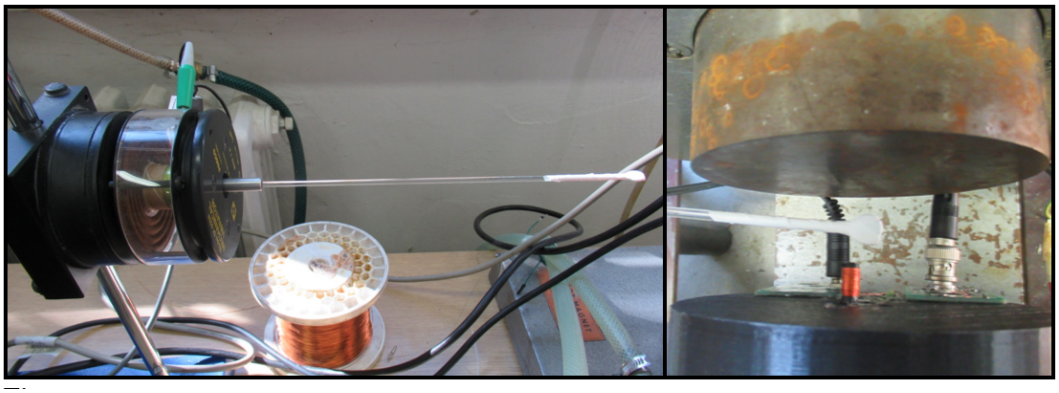

Figure 3.13: Operating Position of the Vibrator Used for the VSM and the Resulting Position of the Sample Within the Yoke's Air Gap

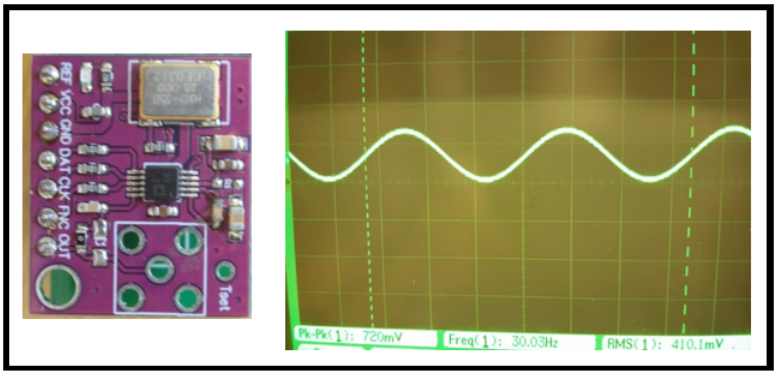

Figure 3.14: The CJMCU AD9833 Board Used in the VSM and its Sinusoidal Output

An accompanying circuit would then need to be designed to address three issues with the DDS. First, as seen in figure 3.14, the output has an offset caused by a DC component of the signal. A passive high pass filter would thus be required to remove it and shift the sine wave back to the zero.

Experimentally, we found that to run the vibrator at a consistent 5mm amplitude at 30 Hz, it required an input of at least 1.25 V_{RMS} at 58mA.

The second issue then was that the output of the AD9833 after the filter was only 0.243 V_{RMS}. Since this voltage is much smaller than the required

voltage, it would be necessary to amplify the signal after the filter. An OP07-based non-inverting amplifier was chosen to handle the amplification. This was done so that there would not be a 180°phase shift at the amplifier output. This would be needed for later parts of the build since any phase shifting could add to the jitter with respect to the reference signal of the lock-in amplifier. It also had the added benefit to ensure there would be a high input impedance in the amplifier as opposed to an inverting setup[18]. The gain of this amplifier was set to 5.5 which resulted in an output voltage of 1.336 V_{RMS} which would be sufficient to supply the required voltage.

The third issue was then to provide the vibrator with the 58mA input current it needed. The OP07 did not have an absolute maximum rating for current output in its data sheet[19]. It was tested experimentally though that it was not capable of sufficiently providing that current for the vibrator. To address this issue, an LT1010 Unity Gain Amplifier with a maximum output current of ±150mA [20] was added after the output of the OP07 as the current source for the vibrator.

Lastly, the same measures taken for reducing noise in the yoke control circuit were used in the vibrator control circuit.

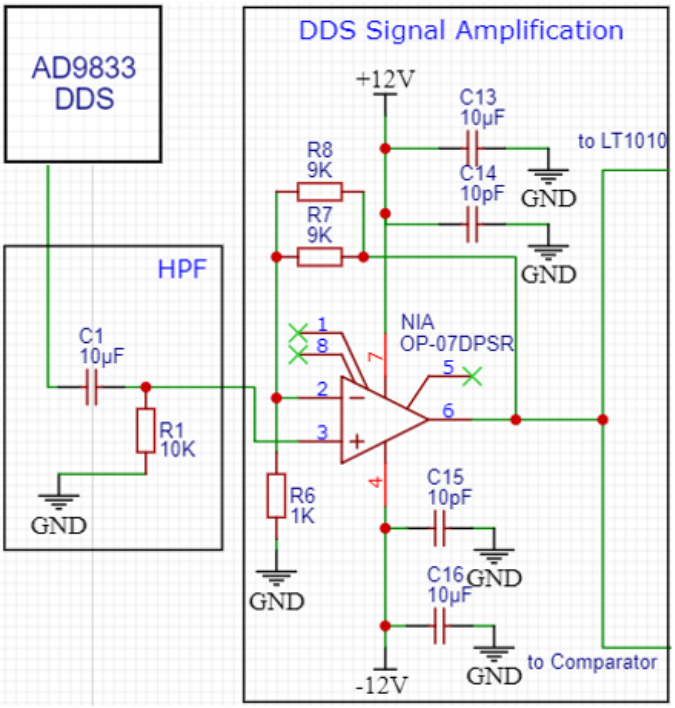

Figure 3.15: The High-Pass Filter and Non-Inverting Amplifier Used in the Vibrator Control Circuit

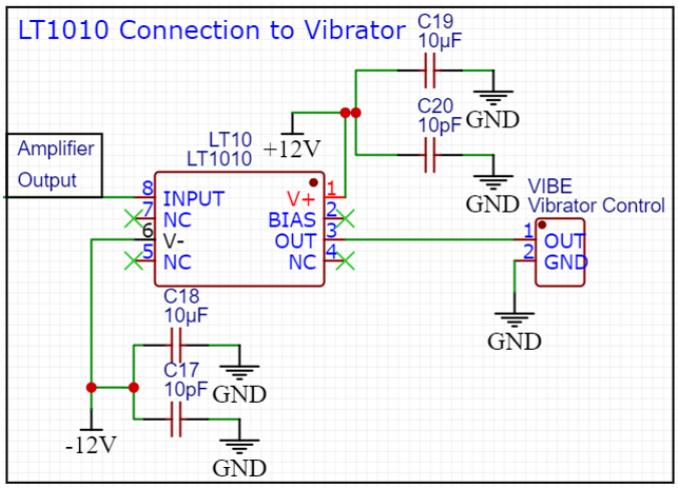

Figure 3.16: The LT1010 Unity Gain Amplifier Used in the Vibrator Control Circuit

3.4 Measurement of Magnetic Moment

Now that there was a means of controlling the applied field, and a means of moving the sample, it was time then to measure the magnetic moment of the sample.

Assuming that the the pickup coil is perfectly short-circuited, the moment of the sample is proportional to the current flowing in it. We used a single pickup coil made with a diameter of 5 mm, a length of 8 mm and 700 turns to measure it. The part of the signal arising from the moment of the sample cannot be precisely measured on its own though since it is buried in high-frequency noise. Thus, it is a common practice to take a reference signal at the same frequency as that of the vibrations and use a lock-in amplifier to demodulate the signal at this frequency[7,9].

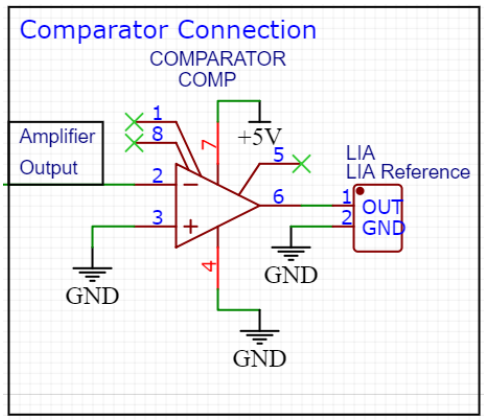

Figure 3.17: Comparator Circuit Used to Create the Reference Signal for The LIA

For our purposes, we used a SR830 Lock-in amplifier(LIA). The filtered output of the AD9833 DDS for the vibrator control was also fed into a MCP6541 comparator to serve as the reference signal for the LIA. The SR830 was set to extract the real part of the signal from the coil to measure the moment of the sample. This would then be sent directly to the computer running the control program via GPIB cable.

Originally, the current from the coil was to be measured directly by the LIA in current mode. But for unidentifiable reasons, the LIA was always indicating that its input was overloaded when being used in current mode. We thus decided to do the current to voltage conversions manually and run the LIA in voltage mode instead. This current to voltage conversion was done using an OP07 op-amp and a 1 MΩ resistor as to not have any issues regarding the internal resistance of the LIA. This issue was found after the main PCB was fabricated so the IV converter was placed on an additional PCB.

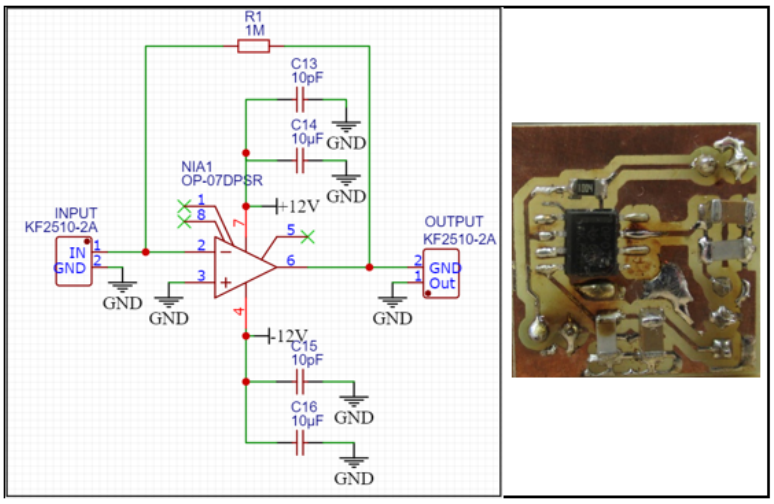

Figure 3.18: Schematic and Additional PCB for the IV Converter

Unlike the measurement of the applied field which is based on a sensor of fixed position with a known characteristic, the magnetic moment measured by the coils is heavily dependent on the positioning of the vibrator and the sample. It would be possible to calibrate these measurements using a sample of well-known magnetic moment but it will be necessary that the vibrator and sample holder remain in the exact same position relative to the pickup coil in proceeding measurements for the calibration to remain accurate. This would not be possible with the current state of the VSM prototype as it still lacks a means of fixing the vibrator to a single position and a means of precisely adjusting its vertical position to a specific value. The calibration of the measured values of magnetic moment will then have to be done on a case-per-case basis for the VSM prototype. A means of doing so had thus been incorporated into the control software.

3.5 Machine Control and User Interface

Now if all the previously elaborated systems are working correctly, they can be used in conjunction with each other to measure the moment of the sample. First, the DDS will have to continuously produce a control signal to power the vibrator and to feed into the reference of the LIA. Next, the yoke will have to be set and the applied field will be measured. Then the LIA output will be read through the GPIB connection. Besides the initial programming of the DDS, the other steps make up the measurement cycle that will have be done each time a point is measured in the hysteresis loop. This would be very tedious and susceptible to error if done manually and could take up a lot of time since many points need to be taken. This is not ideal since the longer it takes to measure the loop, the more susceptible the measurements will be to drift[1]. Thus, in order to improve the user experience when operating the VSM and improve the quality of the results, it would then be necessary to centralize the control of each of the systems and automate them through a control program.

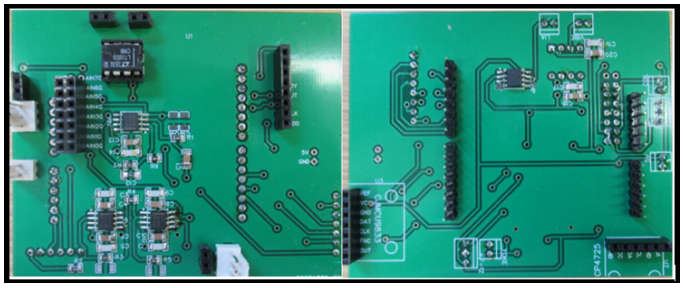

Figure 3.19: The PCB design

A low-cost solution is to use an Arduino Uno and to design a PCB that will attach as a shield to it where the other boards can be mounted on. The Arduino's connections to different parts of the machine can then be used to control the different subsystems via serial communication.

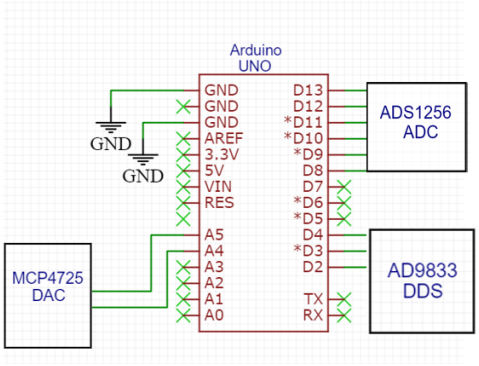

Figure 3.20: Pin Connections Between the Arduino and the Other Components of the VSM

Now that the hardware has been discussed, it is time to take a look at the software that was used to centralize the control and data acquisition of the VSM.

The back end of the control program is written in the Arduino IDE. It handles the primary communications between the Arduino Uno and the other ICs on the PCB. The program was written such that each functionality is handled by their own respective functions based off of open-source libraries for the control of the DDS[21], ADC[22], DAC[23]. The main body of this program is a single switch case controlled by single character serial inputs and the program is set to only output data readings from the hall sensor or the pickup coils.

The Arduino program does not have any user-oriented outputs because its input-output system has been simplified such that LabVIEW can easily control it without any interference from extra unnecessary data being sent over the serial. The user interactions, and the processing and visualization of data will be handled by the front end LabView program.

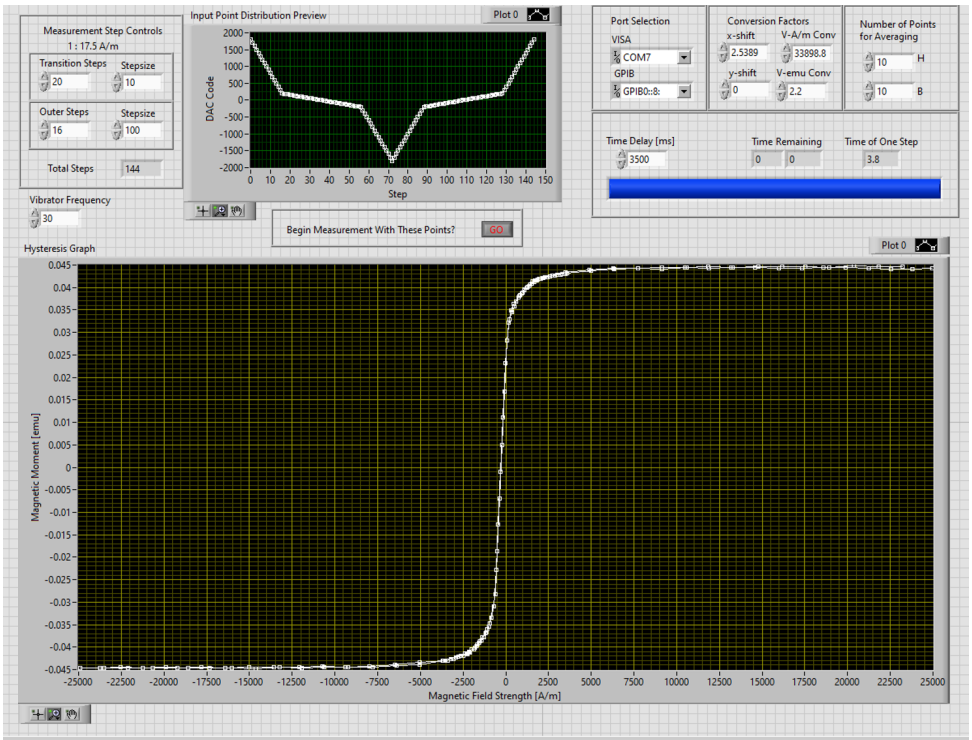

Figure 3.21: The Full Graphical User Interface of the LabVIEW Program

To ensure good loop quality, it is necessary to have more measured points of smaller steps near the transition. Farther from the transition, that is, in saturation, it is sufficient to have fewer points at larger steps as these are usually in the saturation of the material already. The user interface has controls for separately setting the number of steps and step size for points measured close to and far from the transition. After these are set, an array of values for setting the field is created. The values are then plotted on the

preview graph so the user can see their distribution and adjust the controls accordingly before pressing the button to commence the measurement using the generated values.

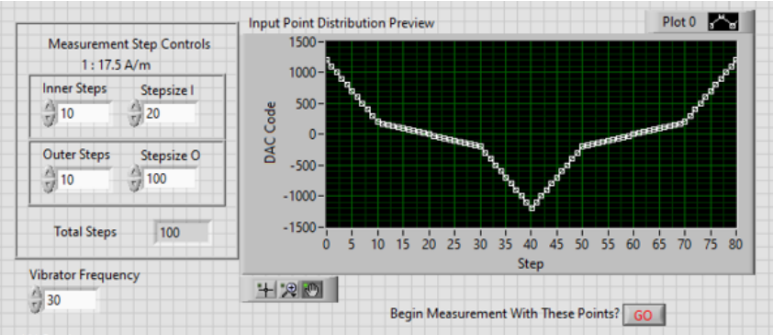

Figure 3.22: The Measurement Step Controls

Since the LIA can be set to measure with different time constants, the settling time, or the time delay between setting the applied field and measuring the magnetization of the sample[1], can be manually set in the user interface of the program. It is recommended to set this time to at least three times the value of the time constant as to ensure that magnetization is measured only after the transient behavior of the LIA has reached steady state.

The yoke polarity still has to be switched manually twice during each measurement of a hysteresis loop. Due to this, the program has been set to pause and show a dialog message whenever manual switching is needed and will not proceed until the user confirms that this has been done.

The user interface also has a set of controls for the processing of the measured data. The first set is used to control the scaling of the loop based on values found through experimental calibration of the VSM and to correct any vertical or horizontal offsets in the results. The second set is used during each time a moment is being measured and controls how many values will be read from the outputs of the ADC and the LIA before storing the average value.

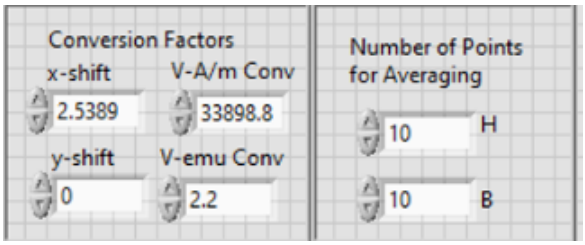

Figure 3.23: The Data Processing Controls

Now that all the controls have been discussed, here is a sample procedure of the measurement of one hysteresis loop:

The user begins by setting the values for all the controls and starting the program. An array will then be created with DAC values based on to the

number of inner points and outer points and their corresponding step sizes. These will follow a hysteresis pattern going from one saturation state to the other and back again. The points in the array will then be displayed on the preview screen and the user can add or remove a number of points before pressing the button to proceed. The first measurement cycle will then proceed and the estimated time till completion will be calculated.

For each measurement cycle, the yoke will then be set based on the current value in the array and the program will wait for the specified time delay to lapse. The measurements of the applied field will then be read from the ADC and averaged accordingly. The same will be done for the readings from the lock-in amplifier read via GPIB. Each point will be plotted on the graph once they are measured as to allow the user to see if there are any issues with the measurements without having to wait for the whole process to finish.

This process will keep being repeated until the program detects a difference in signs between the previous applied value and the upcoming one. If this is that case, a prompt will be given to the user to manually switch the yoke polarity before the program proceeds.

Mathematical correction will then be applied based on the settings on the data processing controls before plotting the final hysteresis loop and saving the data to a csv file.

3.6 Cost Comparison with Commercial VSM

Overall, since the yoke, LIA, and power supplies were readily available in the lab, the total cost for the materials of our VSM was found to be about 9000 Kč with the most expensive parts being the vibrator and the ADS1256 ADC which could still be substituted for a cheaper ADC with lower resolution.

We were not successful in finding the exact prices for buying a brand new commercial VSM as the suppliers would only offer a price quote after discussing the specifications of the VSM that will be ordered. Instead, we decided to compare the cost of our VSM to the listings posted for second-hand units. The cheapest and simplest unit we found was priced at around 48000 Kč while the unit comparable to the commercial VSM in Madrid was priced at around 860000 Kč.

Thus, our proof-of-concept was successful in replicating the operating principle of a VSM for a cost that is significantly lower than the cost of purchasing a VSM.

Chapter 4

Results

It was then necessary to assess the quality of the measurements taken using our low-cost VSM. First, it was necessary to investigate the factors that affect the signal-to-noise ratio of the VSM. Then the magnetic hysteresis measurement for a CoFeSiB amorphous wire taken with our VSM had to be compared to the magnetic hysteresis data measured using the Microsense EV11 commercial VSM. The VSM was then also tested on samples of other materials.

4.1 Stability of the Reference of the Lock-in Amplifier

As stated earlier, the voltage output of the pickup coil needs to be demodulated using a SR830 Lock-in Amplifier. The real part of this signal is then taken as the output which is used to measure the moment of the sample. To do this, the lock-in amplifier requires a reference signal to determine the frequency and phase of the signal that it should take from its input. This reference signal V_{ref} is the output of the Microchip MCP6541-I comparator and is derived from the same sine wave used to control the motion of the vibrator V_{vibe}. This reference needs to be as stable as possible. Otherwise, it can cause a non-negligible change in the angle α between the phasor of the output signal and the real axis. Since the output of our system is dependent on $\cos(\alpha)$ it would be necessary to test the stability of the reference and quantify its effect on the output.

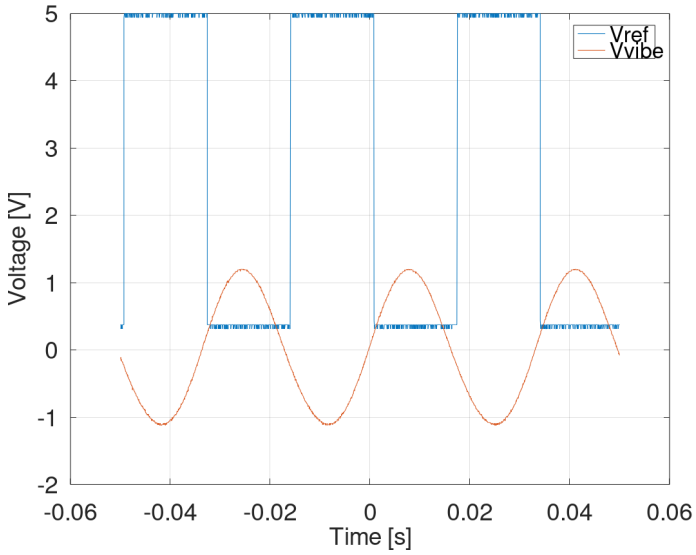

Figure 4.1: Waveform of V_{vibe} and V_{ref} vs. time

To quantify this jitter of the reference signal with respect to the output, V_{vibe} was set as the input of the Lock-in Amplifier and V_{ref} was set as its reference. A LabVIEW program was then taken to measure the phase readings of the lock-in amplifier for 1 minute resulting in the following waveform:

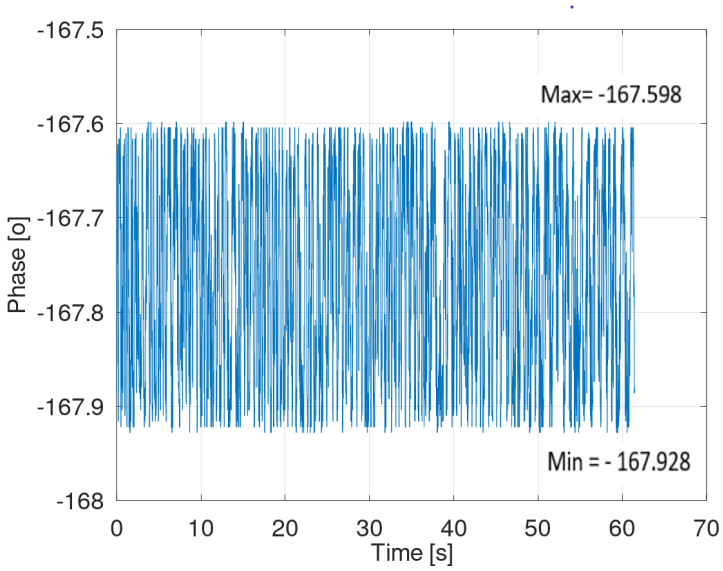

Figure 4.2: Phase Readings of the LIA Taken Over One Minute

The phase values from this measurement attained a maximum value of -167.598°, a minimum value of -167.928°, and a standard deviation of 0.108°. According to the 68-95-99.7 rule, 99.7% of the time V_{ref} will be out of phase with respect of V_{vibe} by about ±0.108° to ±0.324°.

From these values, the maximum the jitter on the output of the system can be calculated as:

$$Cos(0.162°) = 0.9999960028 \tag{4.1}$$

Thus this can cause the real part to change by a factor of

$$1 - cos(0.16) = 4 \times 10^{-6} \tag{4.2}$$

This is small enough to be tolerable for our measurement purposes.

It could be a future possibility to substitute the lock-in amplifier for a demodulator and a phase shifter so it would be useful to quantify how much the LIA contributes to the jitter.

A second jitter measurement was taken without the influence of the lock-in amplifier. This was done by plotting V_{ref} and V_{vibe} on an oscilloscope triggered on V_{ref}. The image was then focused on the rising edge of V_{ref} and V_{vibe} was amplified to better observe how the sine moved relative to V_{ref}.

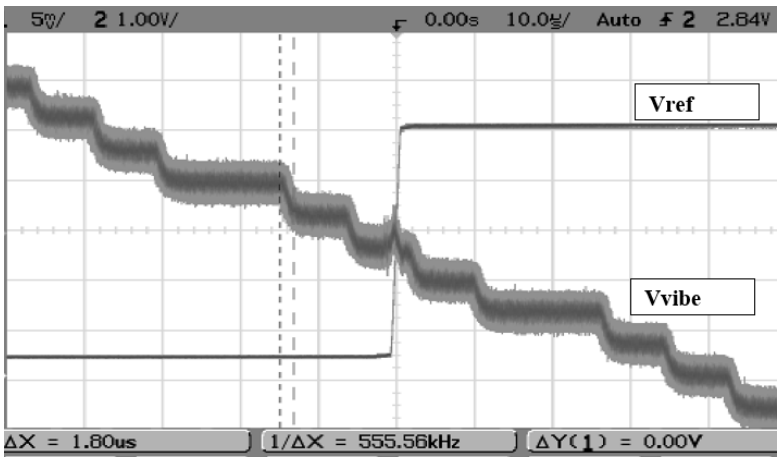

Figure 4.3: Oscilloscope Snapshot of the Jitter of V_{vibe} With Respect to V_{ref}

This jitter was found to be 1.8μs which corresponds to 0.01944° at 30 Hz; one degree of magnitude smaller than the jitter of 0.108° to 0.324°from when the lock-in amplifier was in use. Therefore we derived that the previously observed instability of V_{ref} was caused by the lock-in amplifier and not by V_{ref} itself.

4.2 Noise Reduction Based on Settling Time

Another issue that needs to be addressed regarding the LIA is the transient characteristic of its output due to its internal low-pass filter. It has a time constant(Tc) setting which determines the duration of this transient. Whenever the applied field is set, the LIA output will take about 3Tc before reaching steady state. So ideally, the LIA output should only be read after this time.

Our VSM operates in a discrete sweep measurement method[1]. When using discrete sweep, there is a specified time delay which determines how long to wait before the measurement proceeds after the field is changed[1]. This is set by the "settling time" control in the user interface. It should provide a higher signal-to-noise ratio at the cost of increased measurement time[1] but would need to be tested to determine if it really is necessary.

To test this, the same sample of CoFeSiB amorphous wire was measured twice.

For the first, a hysteresis loop was measured with the following settings:

- 20 small steps with a step size of 200 A/m taken near the transition
- 4 large steps with a step size of 4000 A/m taken near saturation
- In 4 sets, resulting in a total of 96 measured points
- Vibrator Frequency: 30 Hz
- LIA Time Constant: 1s
- **Settling time: 0.5s**

For the second, a hysteresis loop was measured with the following settings:

- 20 small steps with a step size of 200 A/m taken near the transition
- 4 large steps with a step size of 4000 A/m taken near saturation
- In 4 sets, resulting in a total of 96 measured points
- Vibrator Frequency: 30 Hz
- LIA Time Constant: 1s
- **Settling time: 3.5s**

Their comparison can then be seen in the following figures:

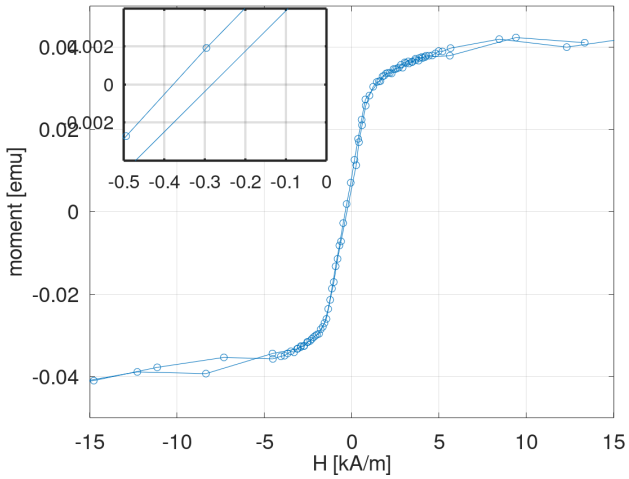

Figure 4.4: 0.5s Settling Time

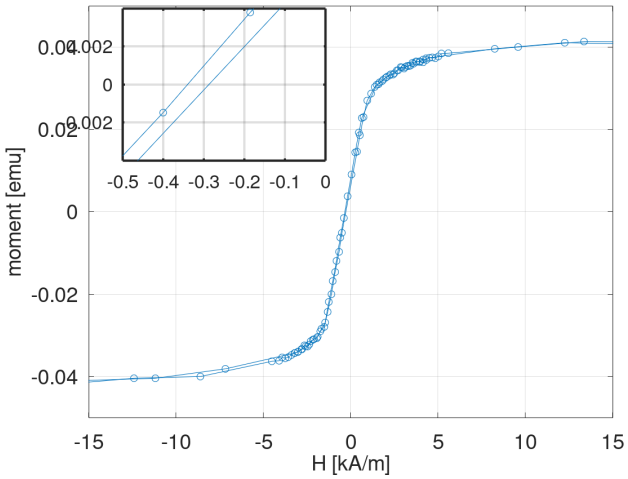

Figure 4.5: 3.5s Settling Time

Past saturation, where less points of larger steps are taken, the measured points deviate much more when settling time is short. Near the transition, more points are taken in smaller steps, yet it can be seen that the short settling time still creates more noise and even gives the loop a larger hysteresis than it should have.

Thus, it is recommended to increase the settling time to at least three times as long as the time constant set in the LIA as it does indeed improve the signal-to-noise ratio of the measurements and the quality of the loop.

4.3 Noise Reduction Based on Averaging

The use of averaging of moment measurements over a longer period of time would also result in a higher signal-to-noise ratio[1]. Since the lock-in amplifier's reading takes time to reach steady state, if only a single point is measured for each moment, premature measurements would lead to errors. Taking the average of multiple points over a set time frame would not eliminate this problem as much as a sufficiently long settling time would. Nonetheless, it would alleviate the problem of premature measurements as taking their average with points measured at steady state would at least bring the final value closer to the steady state value.

To test this, the same sample of CoFeSiB amorphous wire was measured twice.

Two hysteresis loops were measured with the following settings:

- 20 small steps with a step size of 200 A/m taken near the transition
- 4 large steps with a step size of 4000 A/m taken near saturation
- In 4 sets, resulting in a total of 96 measured points
- Vibrator Frequency: 30 Hz

- LIA Time Constant: 1s
- Settling time: 0.5s
- **Averaging: 5 point / 10 points**

They were kept at the same settling time of 0.5s so that any observable noise reduction would be distinguishable from the noise reduction achieved by selecting an appropriate settling time. The tests were then administered with averaging times of 0.5s and 1s, taking 5 and 10 points per moment respectively.

Their comparison can be seen in the following figures:

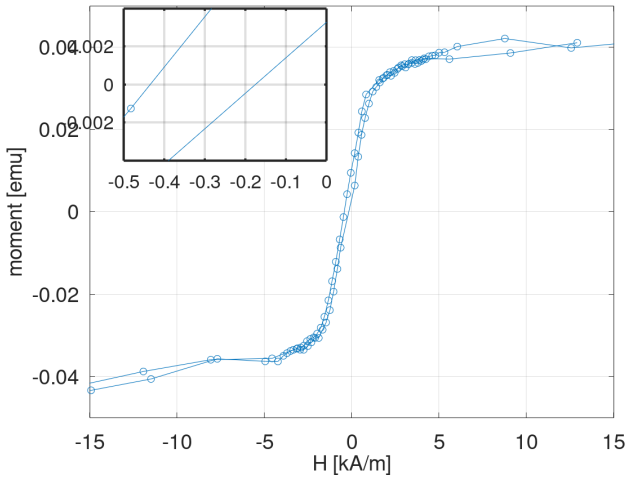

Figure 4.6: 3.5s Settling Time

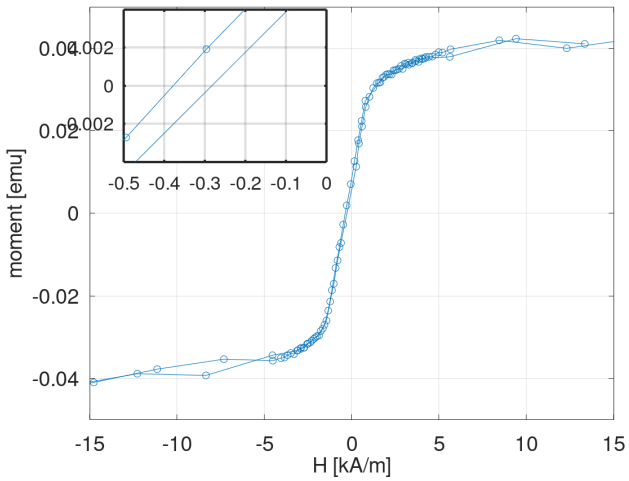

Figure 4.7: 0.5s Settling Time

It can be seen from the plots that with less averaging, the noise-induced false hysteresis worsens. This indicates that more points from the longer

averaging time were taken after the field reached steady state if the averaging is higher. Though this still was not enough to reduce the noise in the saturation region as well as the longer settling time did. Thus, increasing the number of averaged points does indeed improve the signal to noise ratio but it is not as effective as increasing the settling time.

It could also be possible to take even more points per measurement to be averaged. Nonetheless, as long as a few prematurely measured points are part of the average, the improvement could be negligible when adding more points in the steady state region. Which may still make this method less time-efficient than setting a longer settling time but this will need to be tested in further studies.

The use of averaging of a few points per moment still does improve the signal-to-noise ratio so we would still recommend that the controls for changing settling time and averaging points should both be used when measuring samples with our low-cost VSM, but settling time must be prioritized.

4.4 Frequency Dependence of Readings

It was also necessary to test the influence of the vibrator frequency on the output of the system. This would determine if the pickup coil was actually short-circuited and that the impedance of the coil could be considered negligible.

If this were to be true, then the output would depend on the current which produces the back field generated to compensate for the field that generated the current in the coil. This would mean that the measured current would thus be proportionate to the amplitude of the field due to the sample's magnetic moment.

If the coil is not short circuited, the output would be based on the voltage induced in the coil. This is instead proportionate to the derivative of the flux, which is dependent on frequency. Thus, the output of the system had to be compared at different vibrator frequencies.

The yoke was set to a value within the saturation of the sample and the LIA was auto-phased. Then a full loop of points was taken using the control program at the default vibrator frequency of 30 Hz and also at 20 Hz and 40 Hz. A measurement was not taken at 50 Hz since the LIA would not be able to separate the signal form the AC transmission line noise.

Three hysteresis loops were measured with the following settings:

- 10 small steps with a step size of 400 A/m taken near the transition
- 9 large steps with a step size of 2000 A/m taken near saturation
- In 4 sets, resulting in a total of 76 measured points
- **Vibrator Frequency: 30 Hz / 20 Hz / 40 Hz**
- LIA Time Constant: 1s

- Settling time: 3.5s
- Averaging: 10 points

These values were then extracted and plotted against each other in the following graph:

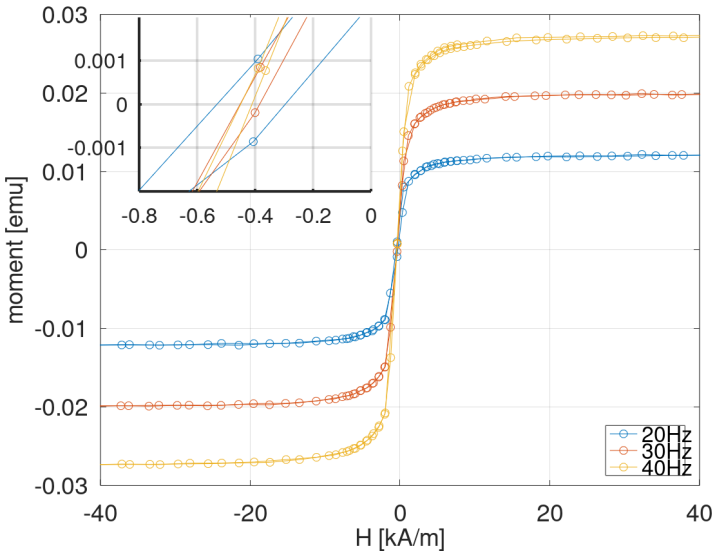

Figure 4.8: Comparison of Hysteresis Measured at Different Frequencies

From this it is observable that the output of the system is indeed dependent on the frequency of the vibrator. Which confirms that the coil is not actually short-circuited and that the impedance of the coil in non-negligible. This dependence creates a gain in the y-component of the plotted hysteresis curve. Though the effect is non-negligible, it is still tolerable as it can be easily corrected mathematically within the LabVIEW program through the controls used for adjusting the Y values.

4.5 Comparison of Data with Microsense EV11 VSM

Since the issues regarding the evaluation and improvement of the signal-to-noise ratio of our VSM have been discussed, it is now necessary to determine the feasibility of using this design as a substitute for a commercially produced VSM.

This was to be done by taking the hysteresis data of the CoFeSiB amorphous wire obtained using the Microsense EV11 VSM and comparing it our VSM's own measurements for the same wire sample.

A hysteresis loop was measured with the following settings:

- 20 small steps with a step size of 200 A/m taken near the transition

- 16 large steps with a step size of 2000 A/m taken near saturation
- In 4 sets, resulting in a total of 144 measured points
- LIA Time Constant: 1s
- Settling time: 3.5s
- Vibrator Frequency: 30 Hz
- Averaging: 10 points

As stated earlier, the calibration of the Y-axis had to be done on a case per case basis, so the calibrations were done based on the hysteresis data obtained from the Microsense EV11 VSM. Once these calibrations were made with the measured hysteresis loop, the following comparison was obtained.

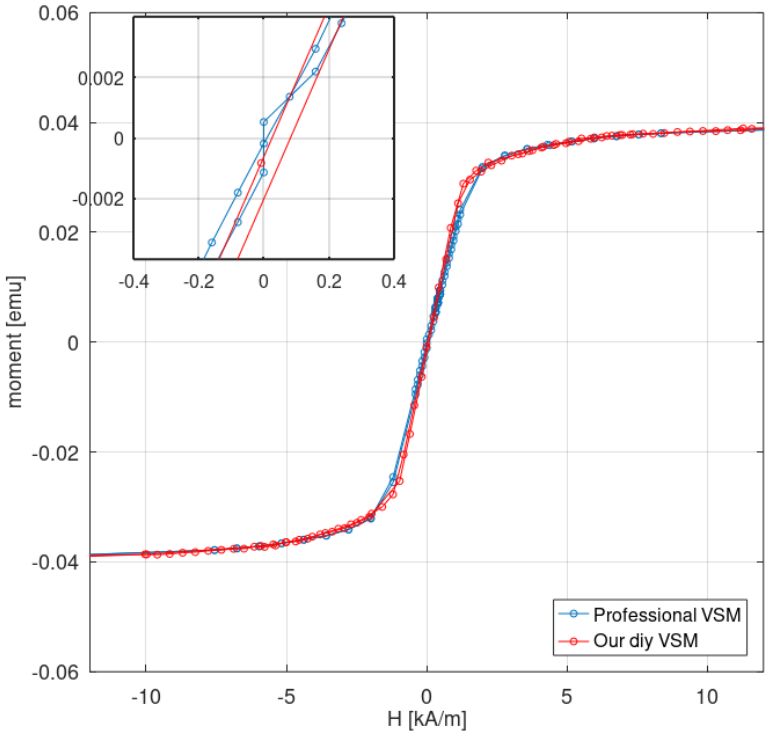

Figure 4.9: The Comparison of The Measured Hysteresis Loop from Our VSM and from Loop Obtained from the Microsense EV11 VSM.

It can be seen in figure 4.7 that the hysteresis loop obtained using our prototype low-cost DIY VSM is congruent with the one obtained using the Microsense EV11 commercial VSM. Albeit, our design's results are still not exact to that of the commercial VSM and still requires proper calibration and more measured points in the transition to precisely quantify the remanence and coercivity. For our purposes of developing a proof of concept, this congruency

is sufficient evidence to support the feasibility of further improving upon this design to later serve as an alternative to purchasing a commercially produced VSM.

4.6 Testing with Annealed Wires

The measurements for the CoFeSiB amorphous wires have proven successful and of sufficient quality compared to those of the commercial VSM. Though since these wires have a very small coercivity of 16.14 A/m we have yet to see how effective the VSM design is in measuring samples with a larger coercivity.

Since CoFeSiB wires of crystalline arrangement exhibit a larger coercivity than their amorphous counterparts[24,25], a sample of CoFeSiB wire was annealed to serve as the test sample. The sample was annealed by running a current through it until it was heated by the Joule effect to its recrystallization temperature and left to cool at room temperature[26]. A quick hysteresis loop was measured with the following settings:

- 16 large steps with a step size of 8750 A/m
- In 4 sets, resulting in a total of 40 measured points
- Vibrator Frequency: 30 Hz
- LIA Time Constant: 1s
- Settling time: 3.5s
- Averaging: 10 points

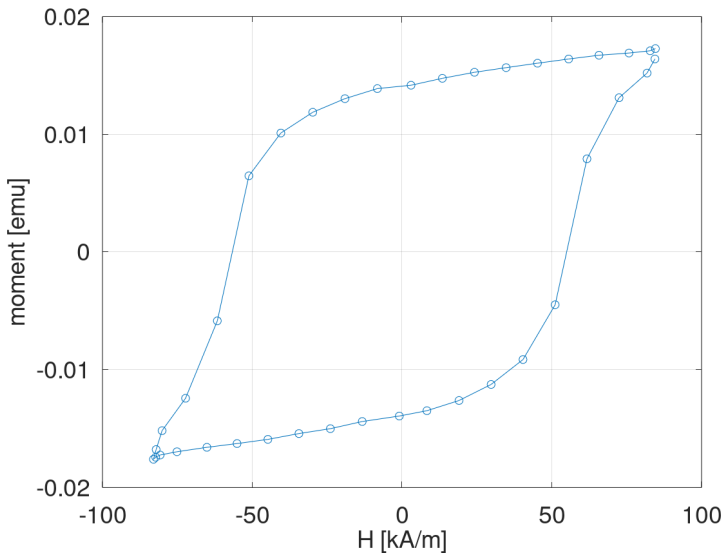

Figure 4.10: Hysteresis Curves Measured for the Annealed CoFeSiB Wires

It can be seen from these plots that the measurement range of the VSM is sufficient enough to measure the coercivity of the sample at around 5.5×10^4 A/m. It is insufficient though for acquiring a proper measurement of the saturation magnetization of the sample. This was because the sample's saturation occurs beyond the linear range of the SS49E Hall Effect Sensor which was no longer able to correctly measure the strength of the applied field.

4.7 Measurement of Nanowires Using the VSM

To further explore the potential uses for the VSM design, measurements were taken for the magnetic properties of Permalloy^{tm} Ni80Fe20 nanowires and compared to measurements taken for them with a SQUID.

This proved to push the design to its limits for two reasons.

First, the sample had a much larger coercivity (about 30kA/m) than the CoFeSiB amorphous wires, and their saturation magnetization was beyond the linear range of the hall sensor. To address this, the hall sensor was not used to measure the field and instead the DAC codes were used. This was possible since the hysteresis of the yoke could now be considered tolerable when compared to the large coercivity of the samples.

Second, the nanowires, being much smaller than CoFeSiB amorphous wires, produced a signal in the pickup coil that was smaller by a factor of 10. This meant that the noise that was considered negligible in the previous measurements could no longer be considered as such. To alleviate this, the time constant of the LIA was increased to 3s and the settling time was increased to 11.5 seconds. The averaging was also increased to 40 points to help somewhat improve the signal-to-noise ratio.

A hysteresis loop was measured with the following settings:

- 20 large steps with a step size of 4000 A/m
- In 4 sets, resulting in a total of 80 measured points
- Vibrator Frequency: 30 Hz
- LIA Time Constant: 3s
- Settling time: 11.5s
- Averaging: 20 points

Which resulted in the following plot that has been compared with the loop measured using the SQUID:

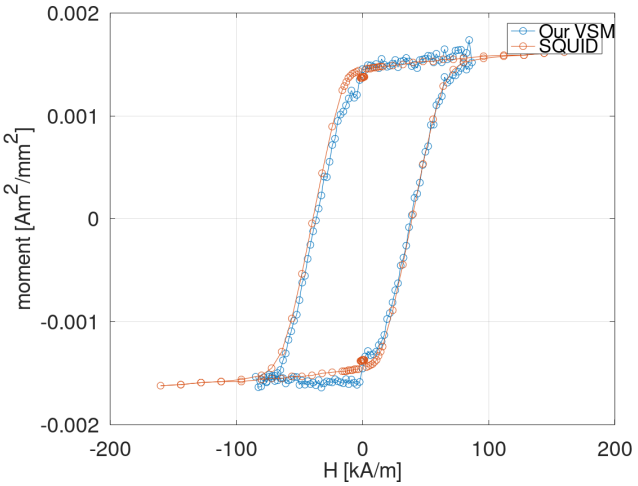

Figure 4.11: Comparison of Measurement of Nanowire from Our VSM and the SQUID

It is visible that even with the extended range, only a measurement of a minor loop was possible due to the limitations of the DAC output so not enough points could be precisely measured in saturation. It is also visible that even with the longer time constant and higher averaging, the readings are still much noisier since the small signal due to the size of the wires greatly affecting the signal-to-noise ratio.

This application of the VSM design still has potential though since the SQUID measurements for these nanowires take a few hours and require scheduling a week in advanced. If the noise can be further reduced, the VSM can at least be used for taking initial measurements of the coercivity of the samples before they are taken to be measured using the SQUID.

4.8 Testing of Demodulator as an Alternative to the LIA

As stated earlier, there was a possibility to use a demodulator as an alternative to the LIA. This could be beneficial by reducing the overall size and cost of the entire VSM setup and could solve the issue of the noise caused by the jitter of the LIA's reference signal at low frequency.

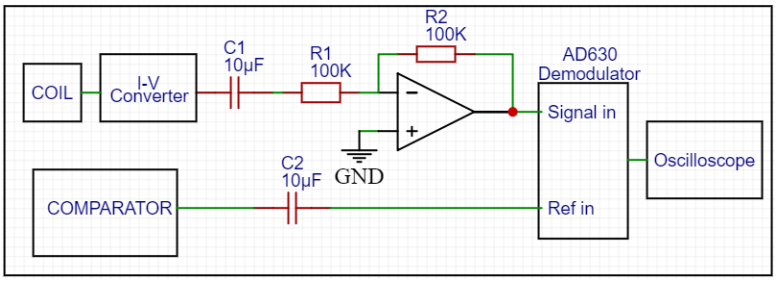

Figure 4.12: The Schematic of the Demodulator Circuit

We chose to use a AD630 demodulator since it was part of a pre-assembled circuit(fig 4.10) in the lab and we were short on time to build our own. The circuit was to be tested with a sample of CoFeSiB amorphous wire to see if using it instead of the LIA would cause any issues with the measurements.

The demodulator still takes its reference from the output of the comparator. While the input of the circuit comes from the I-V converter. The input and reference signals still had a DC offset that had to be removed by capacitors before they could be used.

The pre-assembled circuit also had an inverting amplifier built into the path the input of the AD630. It was not going to be used for our purposes but could not be removed so it was given equal resistance values to act like a unity gain amplifier instead. This could still be beneficial because it provides a large input impedance for the demodulator.

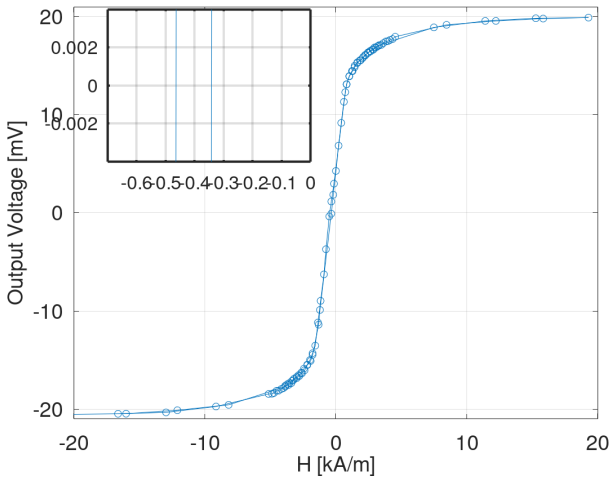

Figure 4.13: Hysteresis Loop of CoFeSiB Amorphous Wire Obtained Using the Demodulator Instead of the LIA

Once it was confirmed that the demodulator circuit was functioning properly, it was time to measure a hysteresis loop of CoFeSiB amorphous wire using the setup with 5 large steps of 2000 A/m and 20 steps of 100A/m. This was done semi-manually with applied field adjustments and measurements were handled by the LabVIEW program while the demodulator output was

recorded manually from the oscilloscope reading. This resulted in graph of figure 4.11.

It can be seen that the VSM still produces a loop of good quality with no drastic shifting or noise being created by the demodulator circuit. It could thus be a viable replacement for the LIA in the future but more testing would be required to confirm this.

Chapter 5

Future Improvements

Our current design for the low-cost VSM has been found to sufficiently measure a loop congruent to that of the Microsense EV11 VSM for the samples of CoFeSiB amorphous wire. This design is still just a proof of concept and there is still much room for improvement of the design of our VSM.

- As earlier stated, a AD630 demodulator could be a sufficient replacement for the SR830 lock-in amplifier but more testing with the demodulator must still be done to confirm this. This could prove beneficial to the future design of the VSM as it would remove the problem with the current mode of the LIA and also the problem with the LIA's influence on the jitter of the reference signal.
- Instead of a basic lab stand, a rigid external frame should be used to hold and position the vibrator. This could also then be given fine adjustment knobs for precisely setting the sample's position relative to the pickup coil.
- The SS49E hall effect sensor is lacking in range to measure samples with larger coercivity and could thus also be replaced with hall sensors with larger ranges such as a TI DRV5057-Q1 [27] with a ±168mT maximum range or a TI TMAG5170A2-Q1 [28] with a ±300mT maximum range.
- The PCB could be redesigned. Mainly to be an all external board wherein the DDS, ADC, and DAC are all incorporated on the PCB and not attached as separate boards.
- A relay could also be added to the yoke for automated switching of the yoke polarity so a full loop can be measured without requiring manual adjustments in between. A control circuit for the relay could also be incorporated into the new PCB.
- It would also be beneficial to construct a power supply circuit for it as not to have to rely on multiple banana cable connections to external power supplies.
- More tests can be conducted on possible means of further improving the quality of the measured loop.

- Tests need to be done on coil size, turn count, and coil positioning.
- The influence of averaging measured points can also be tested further.
- The vibrator should be magnetically shielded to reduce noise due to its magnetic components.
- The OP07 in the I-V converter could be replaced with a LT1007CN8 [29] to reduce the noise due to the amplifier.
- Lastly, it would be worth investigating the effect of using two coils wired in anti-series to eliminate the voltage spikes seen by the LIA created each time the field is changed which could reduce the settling time needed for taking measurements of smaller samples like the nanowires.

Chapter 6

Conclusion

A proof of concept of building a low-cost DIY Vibrating Sample Magnetometer has been successfully developed. This prototype has been successfully constructed using instruments already available in the University's laboratories and an Arduino-based control PCB at a cost of about 9000 Czech Crowns; significantly less than the cost of purchasing even a second-hand commercial VSM. Its measurement capability has been tested through the comparison of its measurements of samples of CoFeSiB amorphous wires to those taken with a Microsense EV11 commercial VSM. These comparisons proved the feasibility of taking magnetic hysteresis measurements with the prototype and its potential to serve as an alternative to purchasing a commercial VSM after further improvements have been made with its design.

Bibliography

[1] G. A.Paterson, X.Zhao, M.Jackson, and D.Heslop, *Measuring, Processing, and Analyzing Hysteresis Data*, Geochemistry, Geophysics,Geosystems **19** (2018), 1925-1945.

[2] D.K. Mahatoa, A. Molakb, and S. Pawlusb, *Impedance, dielectric, and magnetic properties study of La2CrMnO6 ceramics*, Ceramics International **46** (2020), 6368-6376.

[3] L. Li, L. Peng, Y. Li, and X. Zhu, *Structure and magnetic properties of Co-substituted NiZn ferrite thin films synthesized by the sol–gel process*, Journal of Magnetism and Magnetic Materials **324** (2012), 60-62.

[4] F. Cardarelli, *Materials Handbook : A Concise Desktop Reference*, Springer, 2008. 487-510.

[5] D. Jiles, *Introduction to Magnetism and Magnetic Materials*, Chapman and Hall, 1991. 49-52.

[6] D.S. Schmool and D. Markó, *Magnetism in Solids:Hysteresis*, Elsevier Inc., 2018. 3-11, 14-17, 22.

[7] S. Foner, *Vibrating Sample Magnetometer*, Rev. Sci. Instrum. **27** (1956), 548.

[8] J. Fraden, *Handbook of Modern Sensors*, Springer, 2004.

[9] AT.M.El-Alaily, M.K.El-Nimr, S.A.Saafan, M.M.Kamel, T.M.Meaz, and S.T.Assar, *Construction and calibration of a low cost and fully automated vibrating sample magnetometer*, Journal of Magnetism and Magnetic Materials **386** (2015), 25-30.

[10] A. Niazi, P. Poddar and A. K. Rastogi, *A precision, low-cost vibrating sample magnetometer*, Current Science **79** (2000), 98-109.

[11] S.T. Assar and H.F.Abosheiasha, *Structure and magnetic properties of Co–Ni–Li ferrites synthesized by citrate precursor method*, Journal of Magnetism and Magnetic Materials **324** (2012), 3846-3852.

[12] Microchip,*MCP4725*,http://ww1.microchip.com/downloads/en/DeviceDoc/22039d.pdf [Online; Accessed: 2020-05-12].

[13] Texas Instruments, *ADS1256 Very Low Noise, 24-Bit Analog-to-Digital Converter*, https://www.ti.com/product/ADS1256 [Online; Accessed: 2020-07-27].

[14] Quantum Design, *VSM Sample Mounting Techniques*, https://www.qdusa.com/siteDocs/appNotes/1096-306.pdf [Online; Accessed: 2020-07-29].

[15] J. A. Arregi, *Vibrating sample magnetometry*, http://magnetism.eu/esm/2019/practical/VSMpractical.pdf [Online; Accessed: 2020-07-29].

[16] PASCO Scientific, *Mechanical Wave Driver SF-9324*, https://d2n0lz049icia2.cloudfront.net/productdocument/Mechanical-Wave-Driver-Manual-SF-9324.pdf [Online; Accessed: 2020-02-26].

[17] PASCO Scientific, *Mounting The Mechanical Wave Driver*, 1990 [Image; Accessed: 2020-08-08].

[18] G.B. Clayton, et al., *Operational Amplifiers*, Elsevier Science and Technology, 2003. 1-10.

[19] Analog Devices, *Ultralow Offset Voltage Operational Amplifier OP07*, http://www.farnell.com/datasheets/2258633.pdf [Online; Accessed: 2020-05-12].

[20] Linear Technology,*LT1010*,https://www.analog.com/media/en/technical-documentation/data-sheets/LT1010.pdf [Online; Accessed: 2020-05-27]

[21] P.Balch, *Signal Generator AD9833*, https://www.instructables.com/id/Signal-Generator-AD9833/ [Online; Accessed: 2020-05-12].

[22] Flydroid, *ADS12xx Library*, https://github.com/Flydroid/ADS12xx-Library [Online; Accessed: 2020-05-24].

[23] Adafruit, *Adafruit MCP4725*, https://github.com/adafruit/AdafruitMCP4725 [Online; Accessed: 2020-05-12].

[24] C. Vittoria, P. Lubitz, and V. Ritz, *Magnetic properties of amorphous and crystalline GdFe2*, Journal of Applied Physics **49** (1978), 4908-4917.

[25] V. Kumar, A. Rana, M.S. Yadav, and R.P. Pant, *Size-induced effect on nano-crystalline CoFe2O4*, Journal of Magnetism and Magnetic Materials **320** (2008), 1729–1734.

[26] M. McGuire, *Stainless Steels for Design Engineers: Thermal Processing*, ASM International, 2008. 161-171

[27] Texas Instruments, *DRV5057-Q1 Automotive linear hall effect sensor with digital PWM output*, https://www.ti.com/product/DRV5057-Q1 [Online; Accessed: 2020-07-30].

[28] Texas Instruments, *TMAG5170-Q1 3-Axis Linear Hall Effect Sensor With SPI Interface*, https://www.ti.com/product/TMAG5170-Q1 [Online; Accessed: 2020-07-30].

[29] Linear Technology, *LT1007/LT1037*,https://www.analog.com/media/en/technical-documentation/data-sheets/LT1007-LT1037.pdf [Online; Accessed: 2020-08-06].

[30] S. Bourn, T. Mercer, P. Bissell, and M. Vopson, *Development of a Method to Identify in-Plane Anisotropy Axes in Soft Magnetic Materials Using a Standard Vibrating Sample Magnetometer*, IEEE TRANSACTIONS ON MAGNETICS **51** (2015), 11.

[31] S. Foner, *Hall Effect and Magnetic Properties of Armco Iron*, Physical Review **101** (1955), 1648-1652.

[32] J Vankka, *Direct Digital Synthesizers: Theory, Design and Applications*, Helsinki University of Technology, 2000. 8.

[33] K.N. Henrichsen, *Overview of magnet measurement methods*, CERN, 1998. 1-15.

[34] Texas Instruments, *How delta-sigma ADCs work, Part 1*, https://www.ti.com/lit/an/slyt423a/slyt423a.pdf [Online; Accessed: 2020-05-27].

[35] Texas Instruments, *How delta-sigma ADCs work, Part 2*, https://www.ti.com/lit/an/slyt438/slyt438.pdf [Online; Accessed: 2020-05-27].

[36] Analog Devices, *Balanced Modulator/Demodulator AD630*, https://www.analog.com/media/en/technical-documentation/data-sheets/AD630.pdf [Online; Accessed: 2020-05-27].

[37] Microchip,*MCP6541 Push-Pull Output Sub-Microamp Comparators*, https://www.microchip.com/wwwproducts/en/MCP6541 [Online; Accessed: 2020-05-12].

[38] SEC Electronics Inc., *SS49E Linear Hall Effect Sensor*, https://www.alldatasheet.com/datasheet-pdf/pdf/473135/SECELECTRONICS/SS49E.html [Online; Accessed: 2020-05-12].

[39] Analog Devices, *AD9833*, https://www.analog.com/media/en/technical-documentation/data-sheets/ad9833.pdf [Online; Accessed: 2020-03-24].